

Preliminary performance analysis using the PPP-RTK service of the National Land and Mapping Center in Taiwan

Jiun-Yo Lin^{1*}, Chien-Hsun Chu¹, Feng-Yu Chu¹, Kai-Wei Chiang², Meng-Lun Tsai²

¹ Department of Geomatics, National Cheng Kung University, Taiwan – (f64091122, 11303040, fychu)@gs.ncku.edu.tw

² Department of Geomatics, National Cheng Kung University, Taiwan – (kwchiang, taurusbryant)@geomatics.ncku.edu.tw

Keywords: Extended Kalman Filter, Tactical-grade Embedded GNSS/INS System, GNSS challenges, Initial Alignment, Time Synchronization.

Abstract

Low-cost navigation and positioning systems have become a prominent research field in recent years. In the autonomous vehicle domain, real-time accurate vehicle position determination within lanes is essential for high-level autonomous driving. Regarding real-time performance, while (Precise Point Positioning-Real Time Kinematic)PPP-RTK's corresponding accuracy is not as high as Network-RTK (NRTK), PPP-RTK can provide rapid positioning solutions with a single antenna and single Global Navigation Satellite System(GNSS) receiver. It also features lower bandwidth requirements and unidirectional transmission capabilities than NRTK, allowing more simultaneous users. This makes it a reliable choice when server-side hardware, software, and bandwidth resources are limited. In open-sky environments, autonomous vehicles often rely on GNSS for positioning. However, GNSS signals in urban canyons are susceptible to multi-path effects and NLOS (Non-Line-of-Sight) issues, leading to decreased positioning accuracy. Sensor fusion is the most common solution for maintaining real-time, robust, and high-precision navigation quality across various environments. This research proposes an integration of PPP-RTK and Inertial Navigation System (INS) framework to construct a real-time robust navigation system by integrating PPP-RTK and IMU data using an Extended Kalman Filter (EKF). The experimental equipment includes a tactical-grade Inertial Measurement Unit (IMU) and a low-cost receiver capable of receiving National Land Surveying and Mapping Center (NLSC) correction signals for PPP-RTK functionality. Furthermore, testing was conducted in various challenging outdoor urban environments to validate the proposed algorithm. A high-precision navigation-grade system was used as the reference solution to analyze the accuracy of the proposed real-time navigation system. Additionally, a NovAtel Pwrpak7D-E2 with its internal NovAtel OEM7 receiver utilizing TerraStar service for PPP-RTK implementation was used as a benchmark system to compare the gap between Taiwan's preliminary NLSC PPP-RTK development and existing products. A comparison with NLSC traditional RTK and INS integrated system was also provided. Results show that in GNSS open areas, the 2D Root Mean Square Error (RMSE) between the NLSC PPP-RTK system and EGI-M370 was 2.912 meters lower in accuracy than the benchmark system's 0.585 meters. Although the accuracy of the NLSC PPP-RTK service currently falls below TerraStar's, the system is still in its early development stages. With system parameter adjustment and optimization, it is expected to achieve accuracy comparable to TerraStar, providing a more competitive solution for low-cost autonomous navigation.

1. Introduction

PPP-RTK services have been widely adopted in North America, Europe, and Japan, impacting various sectors including mining, aviation, transportation, geographic information systems, public transit, maritime positioning, and precision agriculture. PPP-RTK reduces the convergence time of traditional systems, yielding numerous benefits including reduced mining machinery errors, enhanced transport navigation reliability, decreased public transit costs, improved agricultural efficiency, reduced maritime fuel consumption, and accelerated GIS data collection. While Network RTK can achieve centimeter-level accuracy rapidly, its high bandwidth communication requirements limit scalability. In contrast, PPP-RTK utilizes low-bandwidth, unidirectional SSR corrections to achieve sub-10 centimeter accuracy within one minute (Hirokawa et al., 2016), making it suitable for mass-market applications such as autonomous vehicle navigation and UAV operations. Recent advances in positioning algorithms benefit autonomous vehicles, which traditionally rely on GNSS, cameras, and radar. However, GNSS may fail under poor signal conditions (Chiang et al., 2013), while cameras perform suboptimally in dynamic situations. Integrating GNSS with INS can enhance positioning accuracy and reliability. Different positioning technologies exhibit distinct characteristics in terms of accuracy, speed, and bandwidth requirements. Single Point Positioning offers rapid processing but lower accuracy, while Precise Point Positioning

(PPP) provides high accuracy but slower processing. Network Real-Time Kinematic (RTK) strikes a balance between speed and accuracy but requires substantial bandwidth, making it unsuitable for large-scale deployment. The PPP-RTK approach combines the advantages of these methods, requiring lower bandwidth and enabling the use of low-cost receivers, making it ideal for autonomous vehicle navigation. In current integration system research, numerous PPP-RTK applications have been developed, including PPP-B2b/INS loosely coupled integration (Xuet al., 2022), PPP-RTK/INS tightly coupled integration (Li et al., 2021), PPP-RTK/INS/Odometer tightly coupled integration (Li et al., 2023), and Multi-GNSS PPP-RTK/INS/Vision with a Cascading Kalman Filter (Gu et al., 2022). These algorithms have successfully implemented PPP-RTK/INS in their applications. The first three methods utilize higher-grade GNSS receivers as experimental equipment in conjunction with tactical-grade or low-cost IMUs. Research using low-cost GNSS receivers has also integrated cameras and multiple GNSS antennas; however, this is impractical for autonomous vehicle outdoor navigation applications due to higher costs, making it unfeasible for current widespread implementation. Therefore, this paper presents three contributions:

1. Evaluation of a PPP-RTK/INS integration system using a navigation-grade INS/GNSS navigation system with a single antenna and single receiver

2. Proposal of an NLSC PPP-RTK/INS navigation solution using a single antenna and single low-cost receiver, utilizing EKF for sensor fusion to provide robust navigation results
3. Assessment of the proposed navigation algorithm in three challenging environments: open-sky, GNSS challenging, and GNSS outage conditions

2. Related work

2.1 Network-RTK

To overcome the spatial limitations inherent in conventional RTK technology, the Network RTK methodology was developed as an innovative solution. In contrast to traditional RTK systems that rely on a single reference station, Network RTK technology utilizes a network configuration comprising multiple reference stations (Euler, 2008), exemplified by Continuously Operating Reference Station (CORS) networks. When users operate within the CORS network coverage, Network RTK technology employs sophisticated interpolation algorithms to model distance-dependent systematic errors (including orbital errors, ionospheric delays, and tropospheric delays) based on the user's position relative to surrounding reference stations. This approach effectively mitigates the distance-related constraints associated with conventional RTK systems. However, Network RTK technology retains the Observation Space Representation (OSR) methodology utilized in traditional RTK, consequently requiring significant bandwidth for data transmissions.

2.2 PPP-RTK

The emergence of PPP-RTK technology addresses the need to reduce PPP convergence time for real-time kinematic positioning applications. While PPP-RTK shares fundamental principles with PPP, it incorporates additional correction messages generated by regional CORS (Continuously Operating Reference Station) networks. These corrections encompass satellite orbital errors, satellite clock errors, carrier phase and pseudo-range observation biases, ionospheric delays, and tropospheric delays (Teunissen and Khodabandeh, 2015). This comprehensive correction approach enables PPP-RTK to reduce PPP convergence time significantly. Although PPP-RTK substantially accelerates convergence rates based on PPP foundations, its reliance on regional CORS network data classifies it as a regional service rather than a global service like PPP. In contrast to Network RTK's Observation Space Representation (OSR) approach, PPP-RTK employs State Space Representation (SSR) methodology. SSR offers several distinct advantages over OSR in terms of communication efficiency:

1. **Transmission Architecture:** SSR implements unidirectional transmission, whereas OSR requires bidirectional communication.
2. **Bandwidth Requirements:** SSR operates with significantly lower bandwidth consumption compared to OSR's substantial bandwidth demands.
3. **Error Representation:** SSR individually represents each error component, while OSR combines all error terms into a single aggregate value.

The discrete error representation in SSR eliminates the necessity for dual-frequency observations to mitigate ionospheric delays, theoretically enabling PPP-RTK implementation with single-frequency receivers (Wübbena et al., 2005). SSR correction messages can be disseminated through both internet infrastructure and L-band communication satellites.

This dual transmission capability ensures that users can receive SSR corrections even in locations with limited internet connectivity, such as mountainous regions and maritime environments.

2.3 GNSS/INS Integration Scheme

2.3.1 GNSS/INS Loosely Coupled Integration

A common GNSS/INS loosely coupled (LC) architecture is illustrated in Figure 1. The GNSS receiver first acquires observational data from satellites, including GNSS ephemeris, pseudo range, Doppler shift, and other related information. These data are processed by the Kalman filter inside the GNSS receiver, which then computes the position, velocity, and time (PVT solution) along with the corresponding covariance matrix. Additionally, the GNSS receiver estimates clock errors.

In the loosely coupled framework, the PVT solution generated by GNSS serves as an observation input to the integrated INS/GNSS Kalman filter, where it is fused with the position, velocity, and attitude computed by the inertial measurement unit (IMU). This process leverages Kalman filtering to integrate information from both GNSS and IMU, thereby enhancing the accuracy and robustness of the navigation solution. Furthermore, the integrated system incorporates an error estimation mechanism that feeds back the GNSS/INS fusion results to the INS for correction, improving positioning accuracy. To ensure the availability of the navigation solution, GNSS must track at least four satellites; otherwise, the PVT solution may become invalid, compromising the stability of the integrated navigation results.

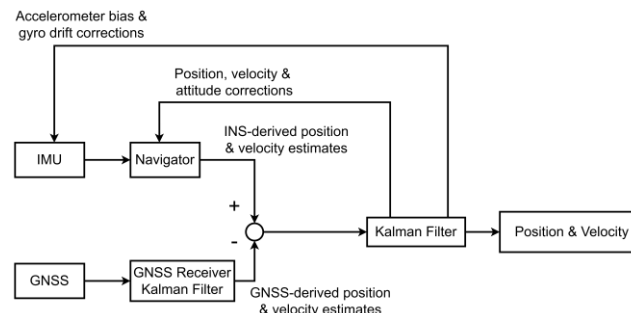


Figure 1. Diagram of common GNSS/INS loosely-coupled integration.

2.3.2 PPP-RTK/INS Tightly Coupled Integration

A PPP-RTK/INS tightly coupled (TC) architecture is illustrated in Figure 2 (Li et al., 2021). The fundamental inputs required by the system include atmospheric corrections, precise orbit and clock data, GNSS observations, and IMU (Inertial Measurement Unit) data, which consists of gyroscope and accelerometer readings. These inputs serve as the foundation for the integration of Precise Point Positioning (PPP) and Inertial Navigation System (INS), enabling both systems to jointly estimate position and attitude. Among them, atmospheric correlations and precise orbit and clock data are essential external inputs for PPP, ensuring that GNSS satellite signals can achieve high-precision carrier phase solutions. Given these heterogeneous raw measurements, the system first processes them through IMU compensation and INS mechanization, as the gray boxes represent. The IMU compensation phase typically corrects for errors caused by temperature drift, sensor misalignment, or other dynamic environmental factors, ensuring that the gyroscope and accelerometer outputs are more accurate. Subsequently, INS mechanization utilizes the compensated IMU data and applies a pre-established inertial motion model to update attitude, velocity, and position continuously. Since INS relies solely on its own measurements for navigation, it can

maintain relatively smooth and stable results over short time intervals. However, its accuracy degrades over time due to accumulated errors, necessitating GNSS observations for correction. This correction process is indicated by the "Aiding" arrow in the diagram, where GNSS provides positional information to mitigate drift in INS estimates. After undergoing "Data Preprocessing," the measurements proceed to GNSS state prediction and PPP observation equation processing. GNSS state prediction extrapolates the system's GNSS position parameters for the next epoch based on precise orbit and clock data, atmospheric corrections, and other GNSS measurements. Simultaneously, IMU state prediction follows a parallel track, using the results from INS mechanization to predict the next moment's state (e.g., platform attitude, velocity, and position). Subsequently, in the "States Mergence" phase, the system integrates the GNSS and IMU predictions into a unified state vector, considering their respective uncertainties and measurement noise. This fusion is typically achieved using a Kalman filter or its variations. Following this step, the system applies the "PPP Observation Equation" to incorporate actual GNSS measurements into the "Measurement Update" process, refining the merged state estimates. This correction mitigates accumulated INS errors, leading to improved positioning and attitude accuracy. In the "Ambiguity Resolution" block, PPP-RTK processing resolves the integer ambiguities in carrier phase measurements. The system achieves centimeter-level positioning accuracy by applying appropriate algorithms to fix the integer ambiguities. Once ambiguity resolution is successfully completed, the results are combined with the previously merged states and incorporated into the final "Tightly Coupled Integration Solutions" (red box). At this stage, all available measurements are optimally integrated to enhance accuracy further and generate the final refined estimates of position and attitude. Lastly, these computed solutions are fed back into the "IMU Compensation" stage (Feedback mechanism), continuously refining the IMU error model and forming a closed-loop correction system.

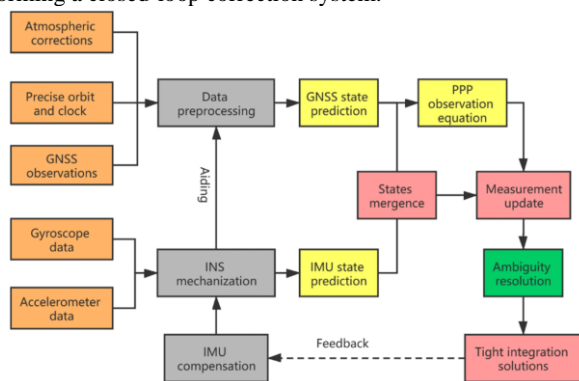


Figure 2. Diagram of PPP-RTK/INS tightly-coupled integration
3. Proposed integration framework for PPP-RTK/INS

The proposed integration framework implemented in this study for navigation applications utilizing NLSC PPP-RTK is illustrated in Figure 3. This framework comprises three primary components: the EGI-M370 inertial navigation module, the Ublox F9P receiver, and the Extended Kalman Filter (EKF). The EGI-M370 module incorporates an accelerometer and a gyroscope to generate position, velocity, and attitude information through the integration of navigation equations (INS mechanization). The corresponding inertial navigation system errors are taken into account, and these states serve as prediction inputs for the EKF module. The Ublox F9P receiver obtains correction data from NLSC through the Networked Transport of RTCM via Internet Protocol (NTRIP) service,

generating position information along with its associated standard deviation. These data are subsequently fed into the EKF module for measurement updates. The comprehensive framework demonstrates the integration process of Inertial Navigation System (INS) and Global Navigation Satellite System (GNSS) data in PPP-RTK navigation applications, employing the Extended Kalman Filter to optimize navigation state estimation.

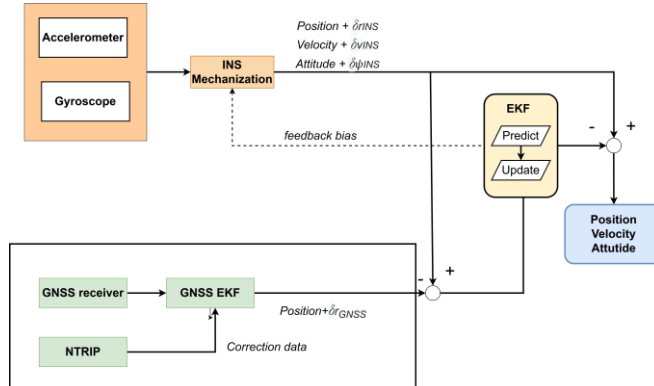


Figure 3. Proposed PPP-RTK/GNSS loosely coupled integration framework

3.1 Error Model

This study implements an INS and PPP-RTK sensor fusion system based on the Loosely Coupled (LC) architecture. To enhance estimation accuracy, an optimal estimator is employed to assess the discrepancies between measured and predicted values, thereby constructing an error model for error estimation. The state vector utilized as the input for the EKF is defined in Equation 1.

$$x_k = [r_{3 \times 1}, v_{3 \times 1}, \epsilon_{3 \times 1}, \omega_{3 \times 1}, f_{3 \times 1}, \Lambda_{2 \times 1}]^T, \quad (1)$$

- where r = position vector
- v = velocity vector
- ϵ = attitude vector
- ω = gyroscope error vector
- f = accelerometer error vector
- Λ = scale factor of gyroscope and accelerometer

4. Experiment

In this research, we employ a ground vehicle as a test-bed to evaluate the performance of the NLSC PPP-RTK and the proposed algorithm. To ensure comprehensive validation, we conduct experiments in three different scenarios around the National Cheng Kung University campus: open-sky conditions, GNSS-challenging environments, and GNSS outage situations, as illustrated in Figure 4.

The GNSS receiver and IMU used to test the proposed PPP-RTK/GNSS navigation system are the Ublox F9P and the EGI-M370, respectively. For comparison with the NLSC, we also implement PPP-RTK using a NovAtel Pwrpak7D-E2 GNSS receiver, which is supported by Terrastar, and employ the EGI-M70 as a benchmark system.

The reference data for this experiment is obtained from the iMAR iNAV-RQH-10018 and the NovAtel OEM7. The specifications of these instruments are detailed in Table 1-3. The experimental setup for this study is illustrated in Figure 5.



Figure 4. Three different experiment scenarios

Gyroscope	
Bias instability	0.8 deg/hr
Angular random walk	0.06 deg/ $\sqrt{\text{hr}}$
Accelerometers	
Bias instability	10 μg
Velocity random walk	0.025 m/s/ $\sqrt{\text{hr}}$

Table 1. IMU Specifications of EGI-M370

Gyroscope	
Bias instability	0.002 deg/hr
Angular random walk	0.0015 deg/ $\sqrt{\text{hr}}$
Accelerometers	
Bias instability	10 μg
Velocity random walk	0.00004 m/s/ $\sqrt{\text{hr}}$

Table 1. IMU Specifications of iMAR-iNAV-RQH-10018

	NLSC	TerraStar
Receiver	Ublox F9P	NovAtel Pwrpak7D-E2
Support format	SPARTN	Customize
Hardware price	350 USD	50000 USD

Table 3. Comparison of PPP-RTK (NLSC) and TerraStar C-Pro

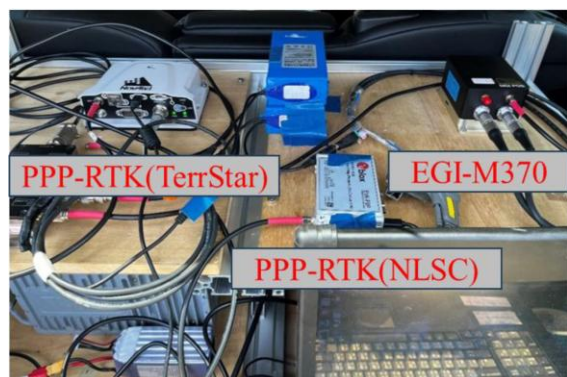


Figure 5. Experimental setup

The red trajectory represents the reference system (iMAR iNAV-RQH-10018), the light blue trajectory represents the EGI-M370 integrated with PPP-RTK (NLSC), the light green trajectory represents the EGI-M370 integrated with RTK, and the orange trajectory represents the EGI-M370 integrated with PPP-RTK (TerraStar). Figure 6 illustrates the corresponding integrated trajectories, where the yellow arrows indicate the driving direction. It can be observed that as the system enters GNSS-denied areas, gradual drift occurs. In certain GNSS-interfered or obstructed areas, the trajectory deviation of the PPP-RTK (TerraStar) integrated solution is larger than that of the PPP-RTK (NLSC) integrated solution. This discrepancy arises because the NovAtel OEM7, being a geodetic-grade receiver, prioritizes accuracy and follows a conservative approach in signal selection (accuracy-oriented), whereas the Ublox-F9P, a receiver designed for general navigation, prioritizes signal availability and adopts a more inclusive satellite selection strategy (availability-oriented). The differences in price and satellite selection logic between these receivers contribute to the observed performance variations in

GNSS-interfered and obstructed environments. In long-duration GNSS outages, the NovAtel OEM7 transitions into a purely inertial navigation mode due to satellite dropout, resulting in greater accumulated errors. Table 4 presents a comparative analysis of the overall performance, indicating that the PPP-RTK (TerraStar) solution outperforms the PPP-RTK (NLSC) solution in open-sky dynamic testing. The analysis results for the three different scenarios are summarized in Table 5. The positioning accuracy analysis in the open-sky scenario indicates that the benchmark system outperforms the proposed system. Specifically, the 3D RMS error, from lowest to highest, is as follows: PPP-RTK (TerraStar), RTK (NLSC), and PPP-RTK (NLSC), with corresponding values of 0.703 m, 0.737 m, and 6.656 m, respectively. In the GNSS interference scenario, the proposed system demonstrates superior performance compared to the benchmark system. The 3D RMS error, ranked from lowest to highest, is as follows: RTK (NLSC), PPP-RTK (NLSC), and PPP-RTK (TerraStar), with corresponding values of 3.506 m, 9.314 m, and 11.123 m, respectively. The key difference between this scenario and the open-sky scenario is that the benchmark system, due to its stringent satellite selection mechanism, rejects GNSS signals that do not meet precision thresholds. As a result, the benchmark system lacks a valid GNSS position solution in interference zones and operates purely in inertial navigation mode, leading to greater accumulated errors. Conversely, the proposed system, which maintains a loosely coupled GNSS-inertial integration, benefits from continuous GNSS updates, resulting in lower positioning errors. Similarly, in the GNSS-obstructed environment, the proposed system consistently outperforms the benchmark system. The 3D RMS error, ranked from lowest to highest, follows the same order as in the GNSS interference scenario: RTK (NLSC), PPP-RTK (NLSC), and PPP-RTK (TerraStar), with corresponding values of 2.418 m, 8.324 m, and 11.525 m, respectively. This behavior aligns with the previous findings, as the benchmark system's geodetic-grade receiver experiences prolonged GNSS signal loss compared to the navigation-grade receiver used in the proposed system. Consequently, the benchmark system relies on inertial navigation for a longer duration, leading to larger accumulated errors compared to the proposed system.



Figure 6. Experimental route

Scenario	Algorithm	Error (RMS)		
		2D (m)	3D (m)	Heading (deg.)
Open Sky	EGI-M370+ RTK(NLSC)	0.721	0.737	0.978
	EGI-M370+ PPP-RTK(NLSC)	2.912	6.656	0.546
	EGI-M370+ PPP-RTK(TerraStar)	0.585	0.703	0.816
Challenging	EGI-M370+ RTK(NLSC)	3.333	3.506	1.887
	EGI-M370+ PPP-RTK(NLSC)	3.535	9.314	0.381
	EGI-M370+ PPP-RTK(TerraStar)	9.226	11.123	0.218
Outage-1	EGI-M370+ RTK(NLSC)	2.270	2.418	5.047
	EGI-M370+ PPP-RTK(NLSC)	2.854	8.324	5.071
	EGI-M370+ PPP-RTK(TerraStar)	9.853	11.525	5.101

Table 4. Performance analysis of NLSC PPP-RTK, RTK and TerraStar PPP-RTK for the whole experiment

Scenario	Metric	EGI-M370 System Comparison		
		NLSC PPP-RTK	TerraStar PPP-RTK	NLSC RTK
Open Sky	2D RMS (m)	2.912	0.585	0.721
	3D RMS (m)	6.656	0.703	0.737
	2D Std (m)	1.138	0.435	0.447
	3D Std (m)	1.838	0.703	0.438
	Heading RMS (deg)	0.546	0.816	0.978
	Heading Std (deg)	0.238	0.861	0.861
GNSS Challenging	2D RMS (m)	3.535	9.226	3.333
	3D RMS (m)	9.314	11.123	3.506
	2D Std (m)	1.603	3.614	2.208
	3D Std (m)	1.838	3.624	2.110
	Heading RMS (deg)	0.381	0.218	1.887
	Heading Std (deg)	0.223	0.168	0.351
GNSS Outage	2D RMS (m)	2.854	9.853	2.270
	3D RMS (m)	8.324	11.525	2.418
	2D Std (m)	1.534	3.958	1.518
	3D Std (m)	0.816	3.803	1.623
	Heading RMS (deg)	5.071	5.101	5.047
	Heading Std (deg)	1.182	1.353	1.218

Table 5. Performance analysis of NLSC PPP-RTK, RTK and TerraStar PPP-RTK in three different scenario

5. Conclusion

For navigation applications, the overall analysis suggests that PPP-RTK (NLSC), utilizing the Ublox-F9P navigation-grade receiver, provides more frequent position solutions in GNSS-interference and obstructed- environments compared to the NovAtel receiver. This ensures better overall navigational control, making its performance superior to PPP-RTK (TerraStar) in such challenging conditions. However, in static tests and dynamic tests conducted in open-sky conditions, PPP-RTK (TerraStar) demonstrates higher positioning accuracy. At present, the NLSC PPP-RTK service is still in its development and adjustment phase and has not yet transitioned into a commercial paid service. With further parameter optimization and system refinement, its accuracy could be significantly improved to a level comparable to TerraStar, enhancing its competitiveness as a strong alternative in high-precision navigation applications.

References

- Chiang, K. W., Duong, T. T., Liao, J. K., 2013. *The Performance Analysis of a Real-Time Integrated INS/GPS Vehicle Navigation System with Abnormal GPS Measurement Elimination*. *Sensors*, 13(8), 10599–10622.
- Gu, S., Dai, C., Mao, F., Fang, W., 2022. *Integration of Multi-GNSS PPP-RTK/INS/Vision with a Cascading Kalman Filter for Vehicle Navigation in Urban Areas*. *Remote Sensing*, 14(17), 4337. <https://doi.org/10.3390/rs14174337>.
- Hirokawa, R., Sato, Y., Fujita, S., Miya, M., 2016. *Compact ssa messages with integrity information for satellite based ppp-rtk service*. *Proceedings of the 29th International Technical Meeting of the Satellite Division of The Institute of Navigation (ION GNSS+ 2016)*, Portland, Oregon, 3372–3376.
- Li, X., Li, X., Huang, J. et al., 2021. *Improving PPP-RTK in Urban Environment by Tightly Coupled Integration of GNSS and INS*. *Journal of Geodesy*, 95, 132. <https://doi.org/10.1007/s00190-021-01578-6>.
- Li, X., Qin, Z., Shen, Z., Li, X., Zhou, Y., Song, B., 2023. *A High-Precision Vehicle Navigation System Based on Tightly Coupled PPP-RTK/INS/Odometer Integration*. *IEEE Transactions on Intelligent Transportation Systems*, 24(2), 1855–1866.
- Wübbena, G., Schmitz, M., Bagge, A., 2005. *Ppp-rtk: Precise point positioning using state-space representation in rtk networks*. *Proceedings of the 18th International Technical Meeting of the Satellite Division of the Institute of Navigation (ION GNSS 2005)*, Long Beach, CA, USA. Held on 13–16 September 2005.
- Xu, X., Nie, Z., Wang, Z., Wang, B., Du, Q., 2022. *Performance Assessment of BDS-3 PPP-B2b/INS Loosely Coupled Integration*. *Remote Sensing*, 14(13), 2957. <https://doi.org/10.3390/rs14132957>.